SUPPLEMENTAL INFORMATIONS

Sonic Hedgehog repression underlies gigaxonin mutation-induced motor deficits in giant axonal neuropathy

Arribat, Mysiak *et al.*

Comprises:

- Supplemental Figures 1-7
- Supplemental movies 1-3
- Supplemental methods

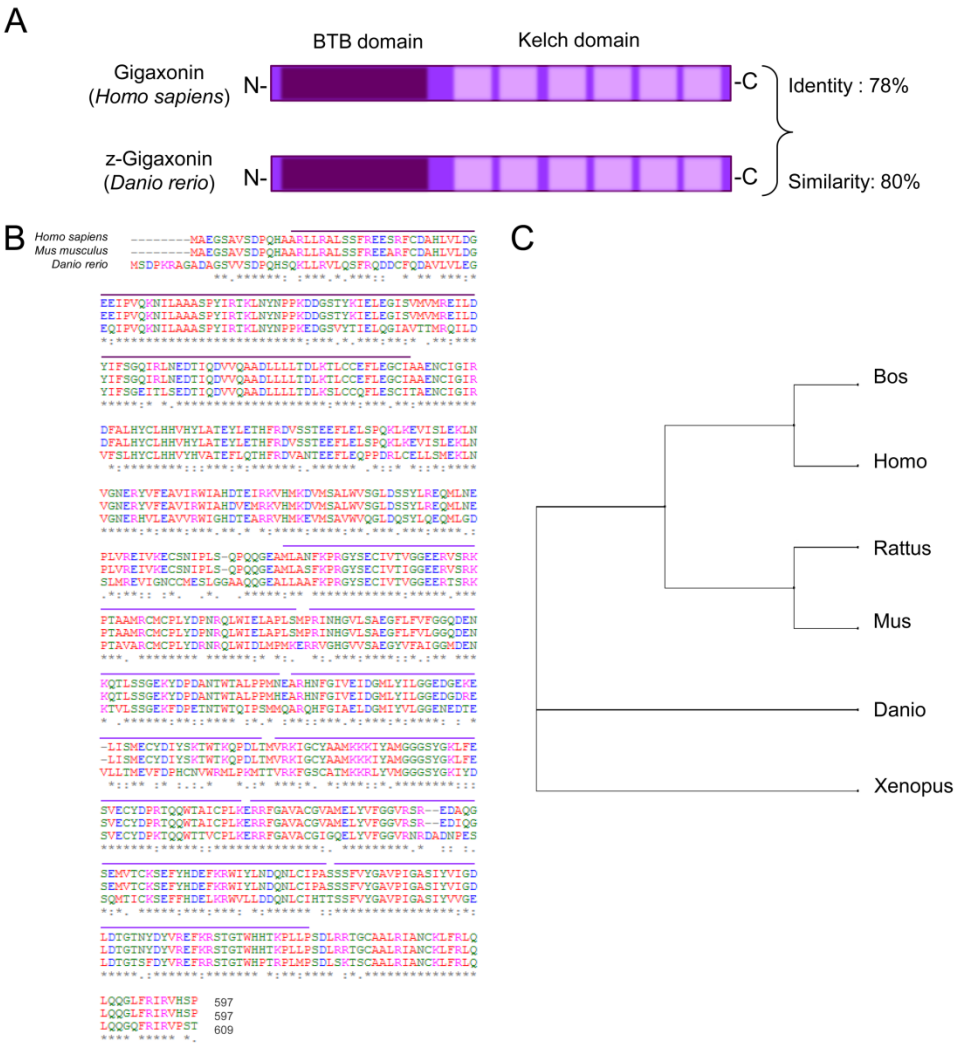

Supplemental Figure 1. Gigaxonin is highly conserved between zebrafish and human. (A) The zebrafish gigaxonin (z-gigaxonin) homolog shares a high identity (78%) with the human protein and presents the same domain organization: a N-terminal BTB domain and a C-terminal Kelch domain. (B) Sequence alignment of human, mouse and zebrafish homologs, with the BTB domain and the 6 Kelch repetitions. (C) Phylogenic tree of the gigaxonin proteins in different species.

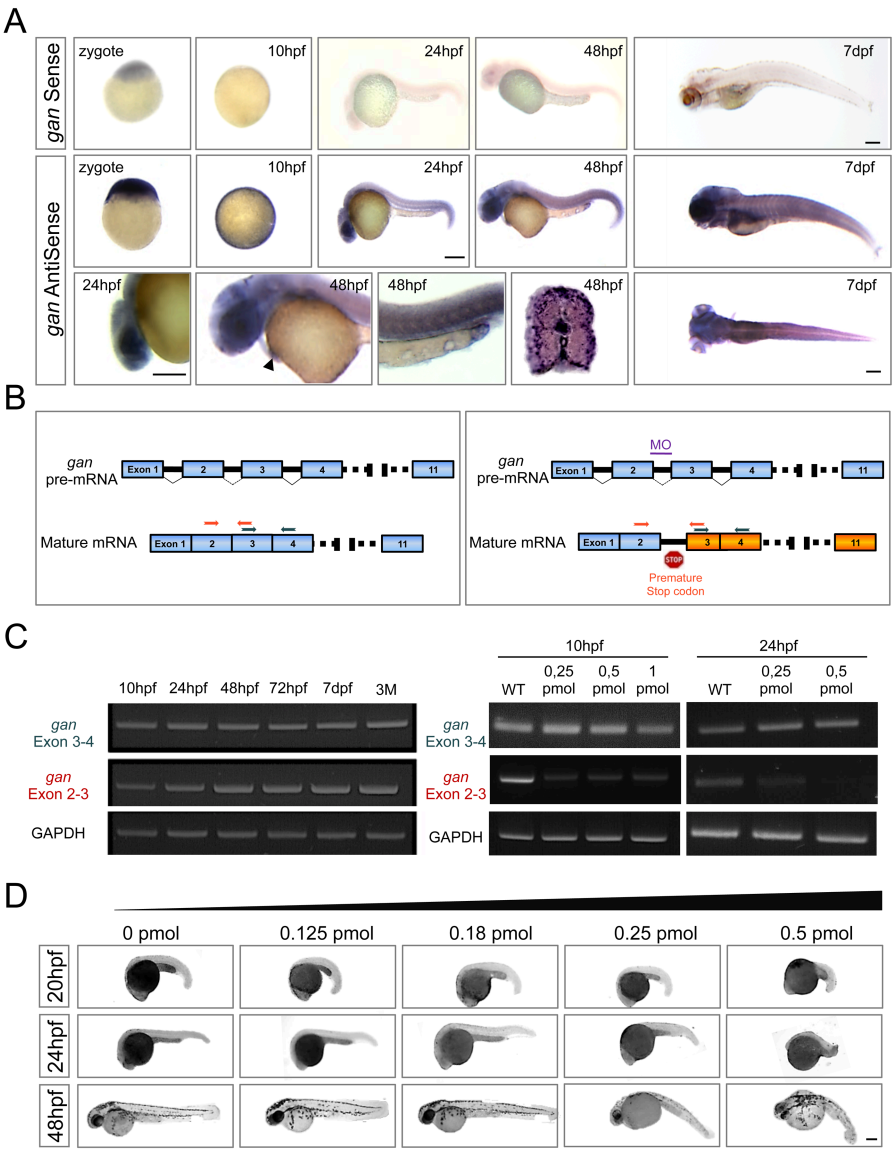

Supplemental Figure 2. Expression of gigaxonin in neuronal tissues and muscles throughout development. (A) Whole-mount *gan* in situ hybridization during embryogenesis, from zygote stage to 7dpf. *gan* transcripts were present early in development in the mesoderm, and were enriched in the muscles, the heart (arrowhead), the eyes, and the notochord (transverse section of the trunk) in zebrafish. (B) Schematic localization of the sets of primers to detect *gan* mRNA (green) and the alteration of its splicing by the morpholinos (red). The morpholinos target the acceptor site of exon 3, causing a premature stop codon within intron 2. (C) Temporal expression of *gan* transcripts by RT-PCR. Left panel: constant expression of *gan* mRNA from embryogenesis (10hpf) to larval (72hpf), juvenile (1 week) and adult (3 months) stages, as assesses by the 2 sets of primers. Right panel: alteration of the splicing of *gan* mRNA from 10hpf and at a minimum dose of 0.25 pmol, as assessed by the reduction of a correct red PCR product. (D) Monitoring of the development of embryos with increasing doses of MO identified 0.25 pmol as the minimum active and non-toxic dose, with no development alteration at 24hpf.

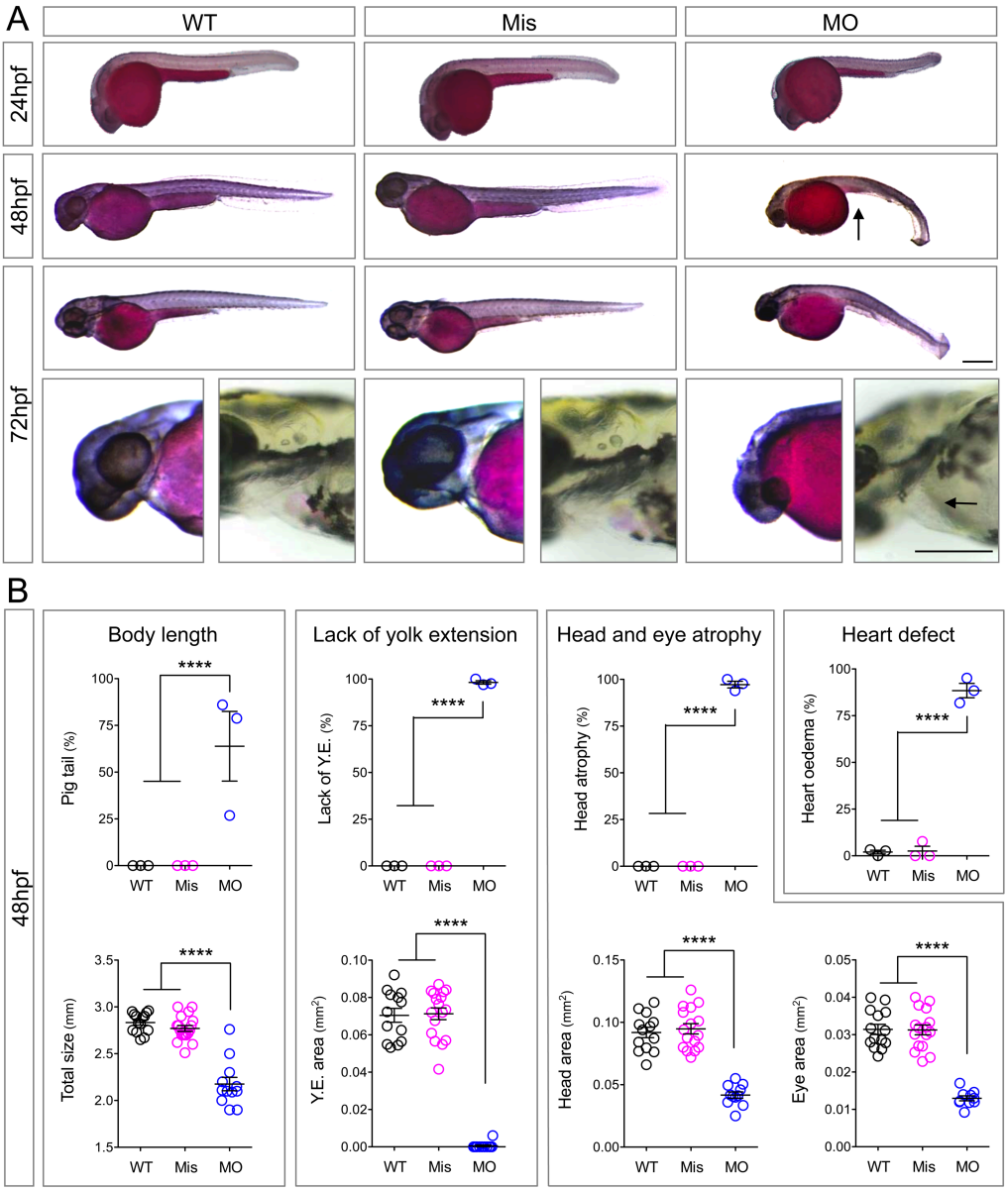

Supplemental Figure 3. Gigaxonin depletion induces neuromuscular abnormalities. (A) Morphological analysis of zebrafish embryos, using hematoxylin/eosin staining. In comparison with non-injected control embryos (WT) or embryo injected with mismatch oligonucleotides (Mis), morphants (MO) exhibit severe morphological alterations from 48hpf, encompassing reduced body length, absence of yolk extension (arrow), head and eye atrophies (higher magnifications), and heart defect (arrowhead in higher magnification). Scale bar: 250µm. (B) Quantification of morphological alterations reveals fully penetrant and severe phenotypes in morphants. The top panels represent the percentage of embryos with the given phenotypes (n=212 (WT), n=147 (Mis), n=117 (MO)) from 3 independent experiments, which are further quantified in the lower panels for n=13-14 (WT), n=16-18 (Mis), n=10-12 (MO). Statistics: upper panels: proportions are compared by the Chi-squared test; lower panels: with normality of the distribution of the data, the parametric one-way ANOVA test (with Bonferroni post-hoc test) was used, and means values ± SEM are represented; **** $P<0.0001$.

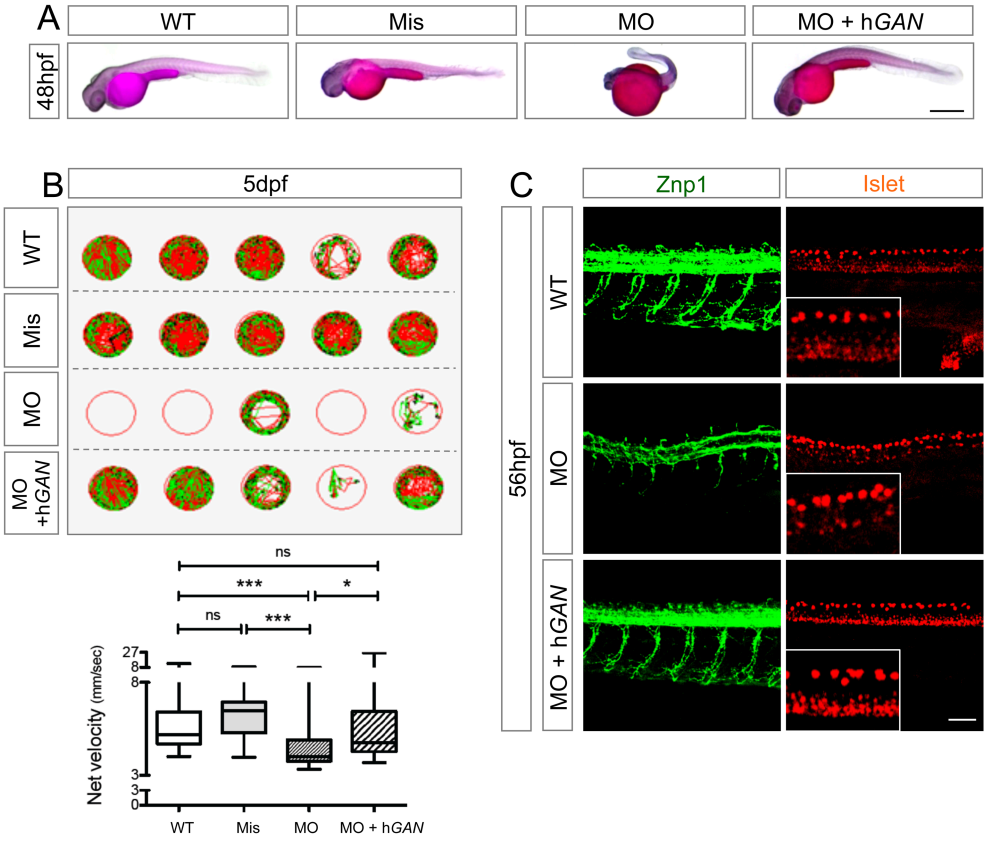

Supplemental Figure 4. The human gigaxonin rescues the morphological, behavioral and cellular deficits of the gigaxonin depleted embryos. Co-injection of 150pg of the human *GAN (*h*GAN)* mRNA with the MO in one-cell stage zygote alleviated the morphological defects in *gan* morphants (A), rescued the locomotor impairment of 5dpf larvae (B) and rescued the pMN axons and sMN deficits (C). The schematic representation of trajectories and the measure of the net velocities show not only a rescue of the motility of most larvae co-injected with the MO and the *GAN* mRNA, but also a restoration of their net velocity, at a level comparable to control larvae; n=68 (WT), n=43 (Mis), n=26 (MO), n=42 (MO+ h*GAN* mRNA). Statistics: in absence of normality of the distribution of the data, a Kruskal-Wallis test (Dunn's post hoc test) was applied; medians with interquartile range, min and max values are represented; ns not statistically significant; * $P<0.05$, *** $P<0.001$. Scale bar in A: 400µm; in C: 50µm.

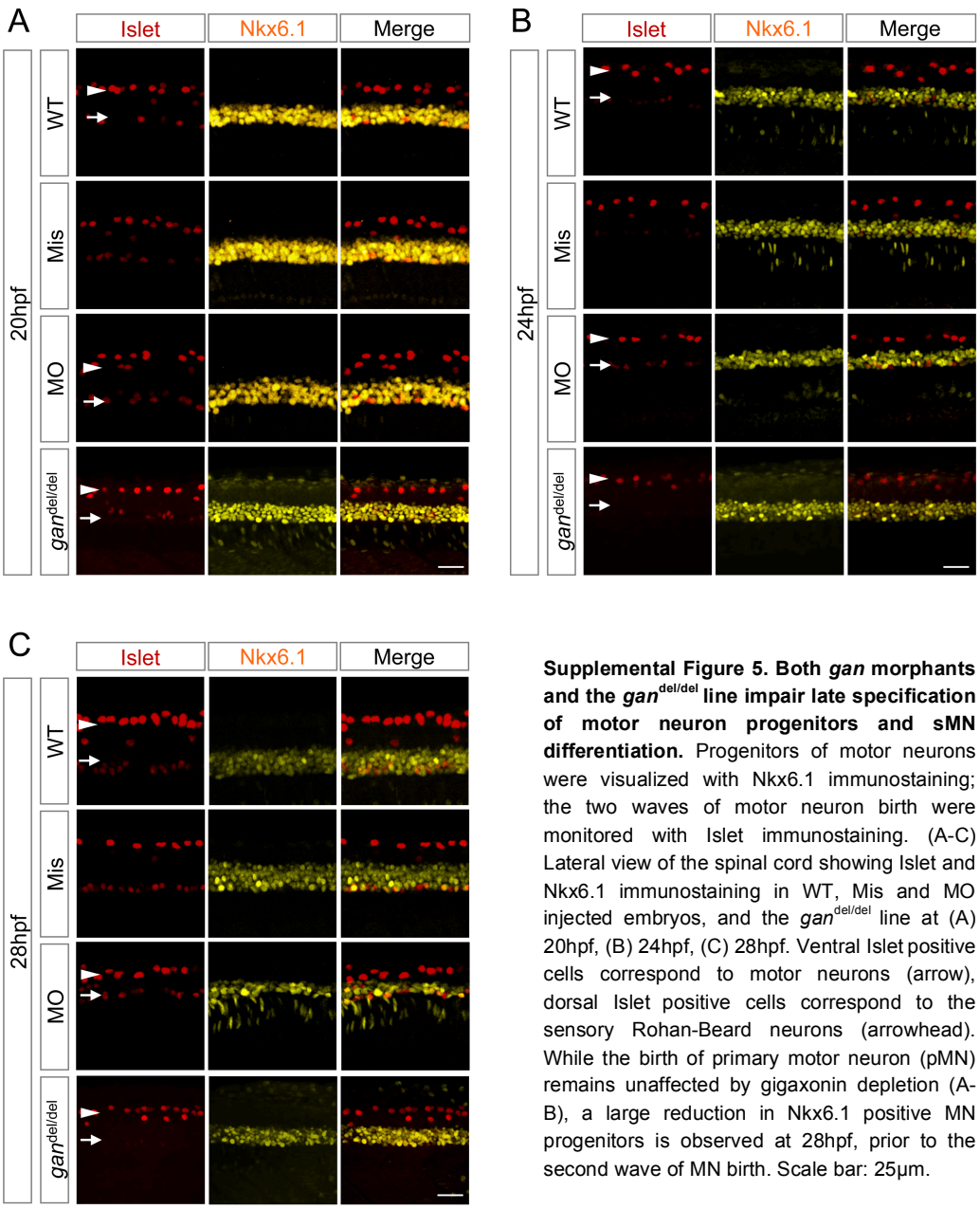

Supplemental Figure 5. Both *gan* morphants and the *gan*$^{del/del}$ line impair late specification of motor neuron progenitors and sMN differentiation. Progenitors of motor neurons were visualized with Nkx6.1 immunostaining; the two waves of motor neuron birth were monitored with Islet immunostaining. (A-C) Lateral view of the spinal cord showing Islet and Nkx6.1 immunostaining in WT, Mis and MO injected embryos, and the *gan*$^{del/del}$ line at (A) 20hpf, (B) 24hpf, (C) 28hpf. Ventral Islet positive cells correspond to motor neurons (arrow), dorsal Islet positive cells correspond to the sensory Rohan-Beard neurons (arrowhead). While the birth of primary motor neuron (pMN) remains unaffected by gigaxonin depletion (A-B), a large reduction in Nkx6.1 positive MN progenitors is observed at 28hpf, prior to the second wave of MN birth. Scale bar: 25µm.

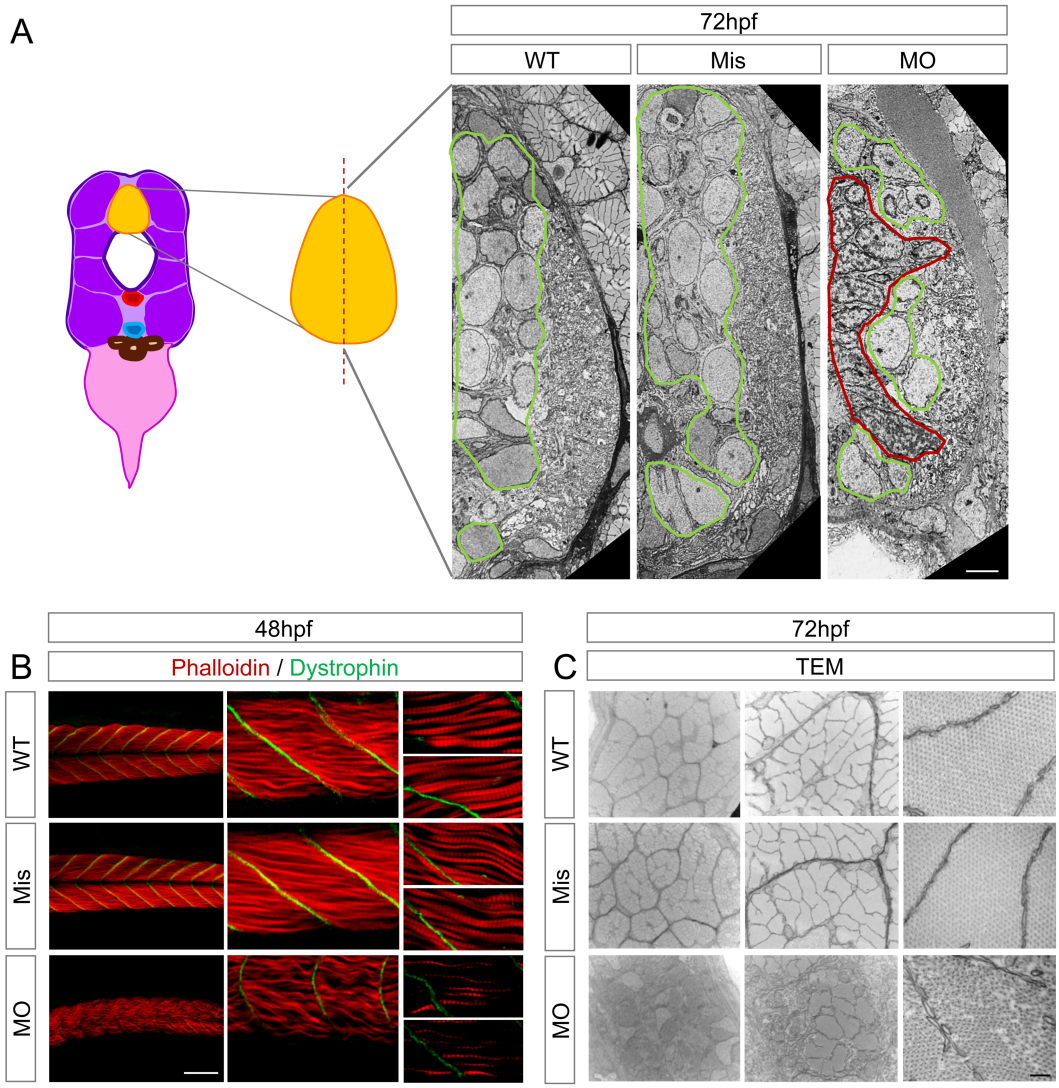

Supplemental Figure 6. Alteration of spinal cord and muscle architecture in gigaxonin depleted embryos. (A) Altered architecture of the spinal cord in gigaxonin depleted embryos. Left: schematic representation of the cross section of a zebrafish, with higher magnification of the spinal cord in yellow. Right panel: Electron micrographs of transverse sections of WT (n=4), Mis (n=4) and MO (n=4) larvae at 72hpf, showing the decreased number of neurons (green area) throughout the spinal cord and glial invasion (red area). (B) Gigaxonin repression alters muscle structure. At 48hpf, *gan* morphants exhibited a severe alteration in the organization and the structure of the somites. In gigaxonin depleted embryos, myofibers were less dense, less compact and wavy (phalloidin-TRITC), the myospetum was absent, and the somite boundaries (as delineated by the dystrophin staining), was barely visible and defined a U-shape, while control embryos presented characteristic V-shape somites. (C) Electron micrographs of transversal sections of 72hpf larvae revealed a deterioration of myofibers with conjunctive tissues invasion in MO animals (left and middle panels). Damaged myofibers exhibited abnormal sarcomeric organization, with an alteration of the normal regular hexameric distribution of actin (thin) and myosin (thick) filaments (right panel); n=4 (WT), n=4 (Mis), n=4 (MO).

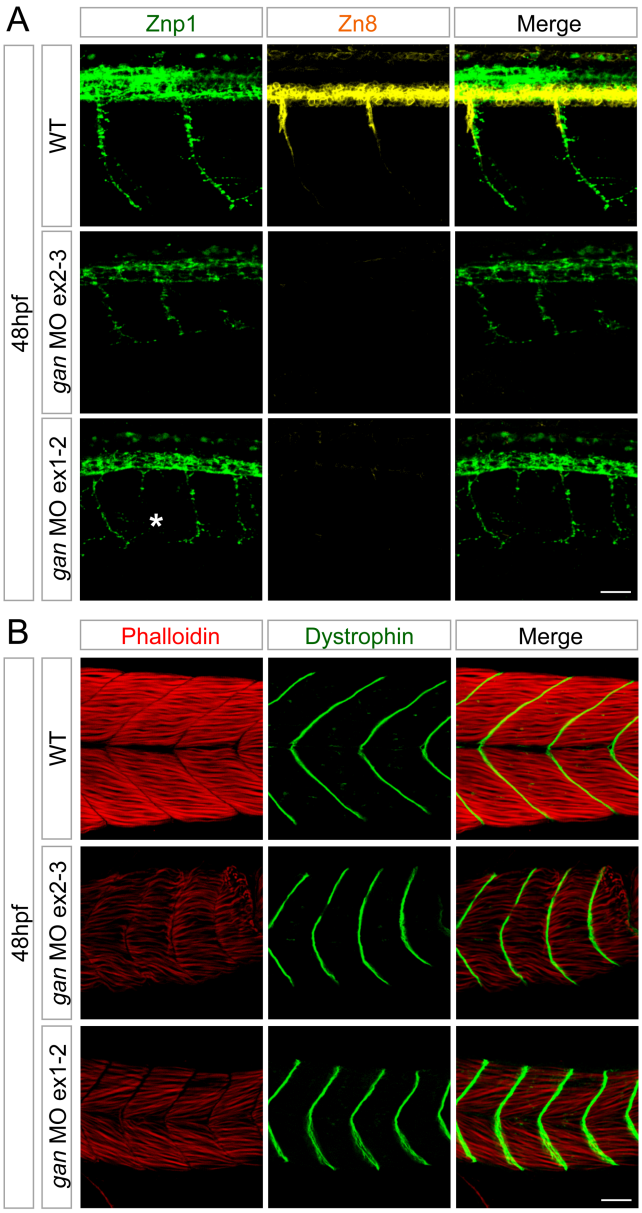

Supplemental Figure 7. Repression of gigaxonin with two distinct MOs reproduces similar motor and muscle deficits. Comparison of the effects of an additional and independent MO (targeting splicing of exons1-2), on the spinal MN (A) and muscle integrity (B) confirms the specificity of the phenotypes for gigaxonin. (A) Similarly to the *gan* ex2-3 MO, the *gan* ex1-2 MO reproduced the absence of sMN (zn8 staining), as well as the alteration of pMN axons (znp1 staining, the white star points to an absent axonal projection) in 48hpf embryos. (B) Injection of *gan* ex1-2 MO mimics the myofiber alteration (phalloidin) and U-shape somites (dystrophin staining) revealed by the repression of gigaxonin using the MO ex2-3 at 48hpf. Scale bar: 25µM.

SUPPLEMENTAL MOVIES

Supplemental movie 1. Motility of control and gigaxonin depleted embryos at 72hpf, upon touch stimulation. The top panel represents the trajectory of a control embryo (non-injected or Mis); the middle and the lower panels correspond, respectively to the looping and pinwheel swimming of gigaxonin depleted embryos.

Supplemental movies 2 and 3. Three dimensional analysis of z-gigaxonin depleted embryos reveals profound alteration of the architecture of the spinal cord in morphants. LightSheet microscopy of MO (bottom) and either control (top) (movie 2) or Mis embryos (movie 3) reveals aberrant structure of the spinal cord upon gigaxonin depletion: altered morphology of the spinal tracts, protruding and absent Cap pMN axons (as revealed by the znp1 marker, in green); and absence of neuromuscular junctions (visualized by the actetylcholine receptors staining using α-bungarotoxin, in red).

SUPPLEMENTAL METHODS

Whole-mount in situ hybridization. Whole-mount RNA in situ hybridization was performed as following: embryos were fixed at appropriate stages in 4%PFA:PBS overnight at 4°C and dehydrated in 100% methanol overnight at -20°C. After gradual rehydration into PBS, the embryos were permeabilized in 10µg/mL proteinase K. The digestion was stopped by 4%PFA:PBS incubation, followed by washes with PBT (0.1% Tween20:PBS) and prehybridization at 70°C for several hours. The embryos were hybridized in sense and anti-sense probes overnight at 70°C. Following high stringency washes through SSC and PBT, the embryos were incubated in anti-digoxigenin-AP, Fab fragments overnight at 4°C. After extensive washes in PBT the embryos were equilibrated in alkaline Tris buffer (100mM TrisHCl pH 9.5, 50mM MgCl2, 100mM NaCl, 0.1% Tween20) and stained in NBT/BCIP until desired color developed. *Gan* sense and antisense probes were amplified by PCR, and directly transcribed thanks to T3 promotor sequence inserted in the forward primers of the probes (see Table 1). *Gan* probe encompassed a 914 base pair region of the *gan* mRNA, from nucleotides 924 to 1838. *Ptch2* antisense probe was a kind gift from P. Huang and A. Schier.

Rescue experiments. The human h*GAN* cDNA was cloned in pcDNA-YFP gateway vector and the corresponding mRNA was produced from the T7 mMessage mMachine Kit (Ambion). Rescue experiments in zebrafish were obtained after co-injection of the MO with 150pg of h*GAN* mRNA.

Full unedited gel for Figure 5 panel B

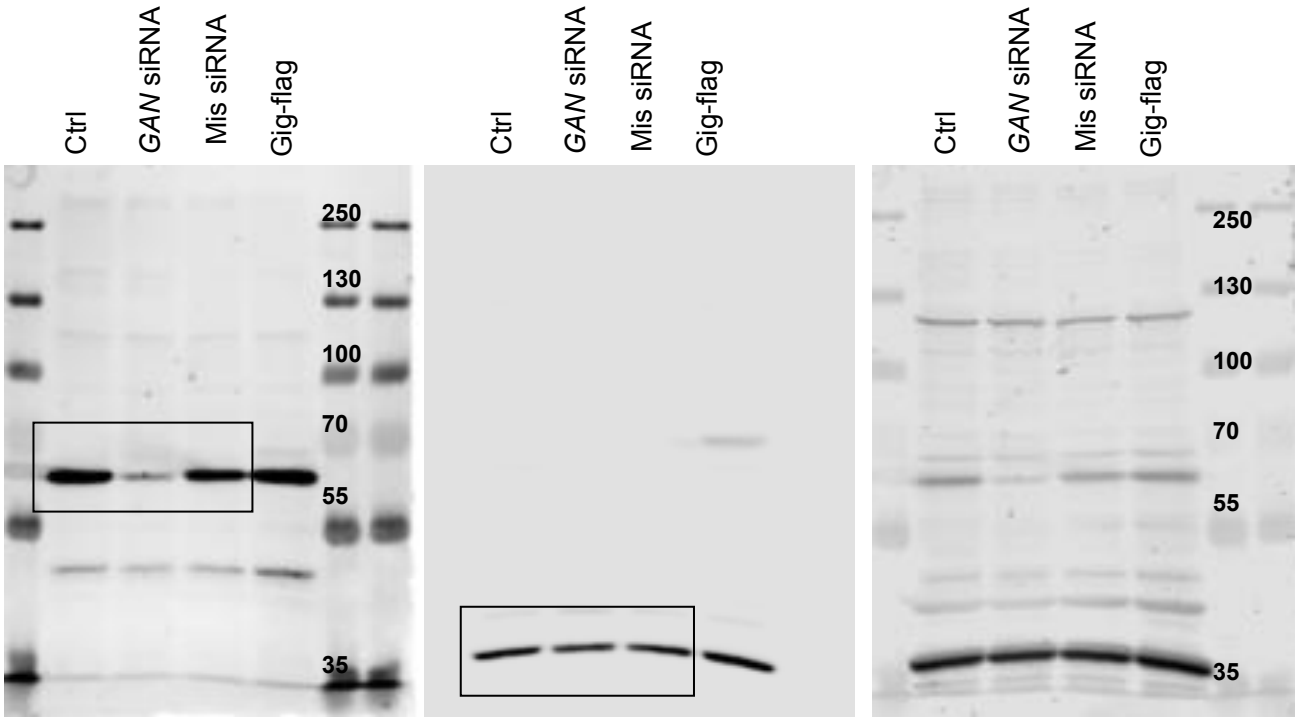

m-α-Gig (1st antibody)
(Biorad system)

m- α-GAPDH w/o ladder

m- α-GAPDH with ladder

Full unedited gel for Figure 7 panel A

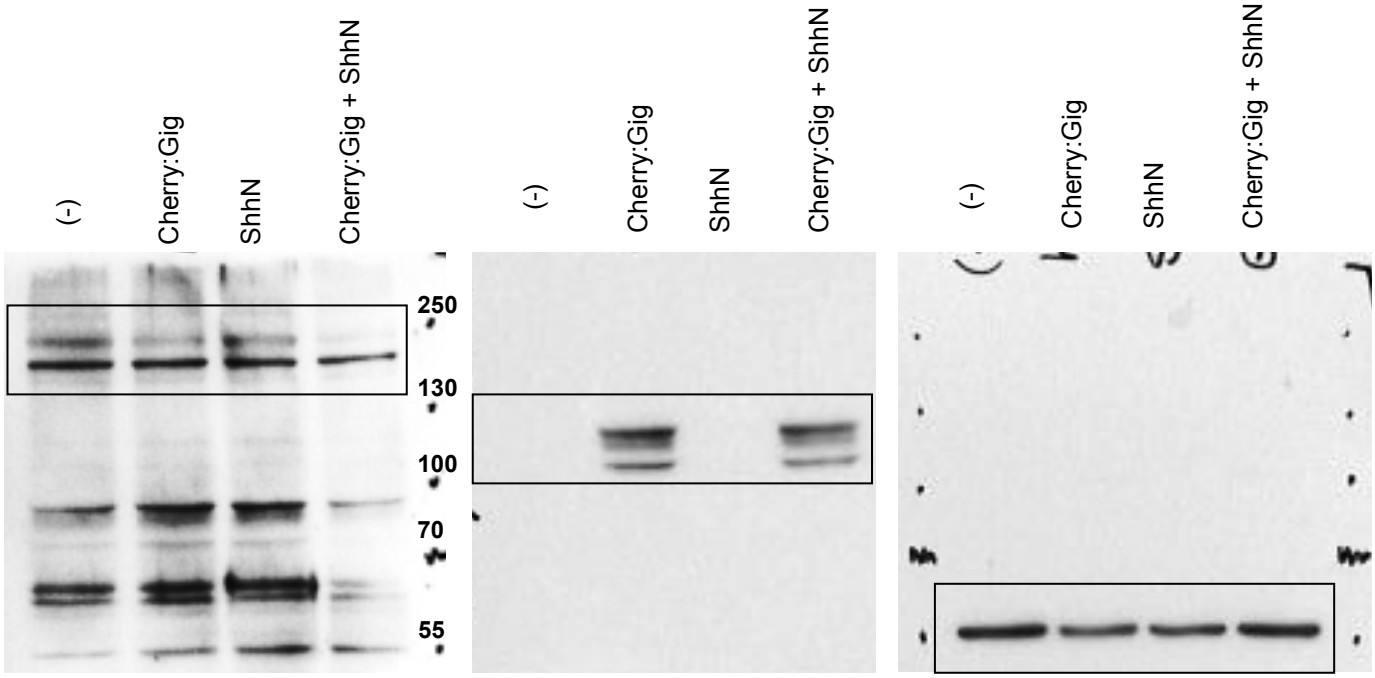

m-α-Ptch (1st antibody)
(conventional developer)

m-α-Cherry (IId antibody)

m- α-Tubulin (IIId antibody)

Full unedited gel for Figure 7 panel B

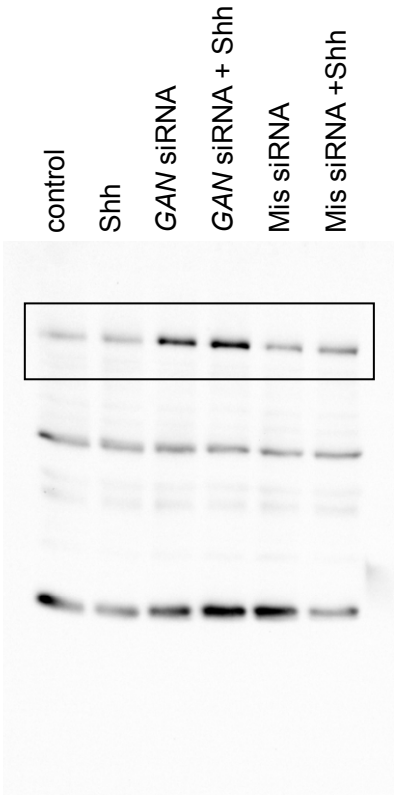

m-α-Ptch (1st antibody)
(Biorad system) w/o ladder

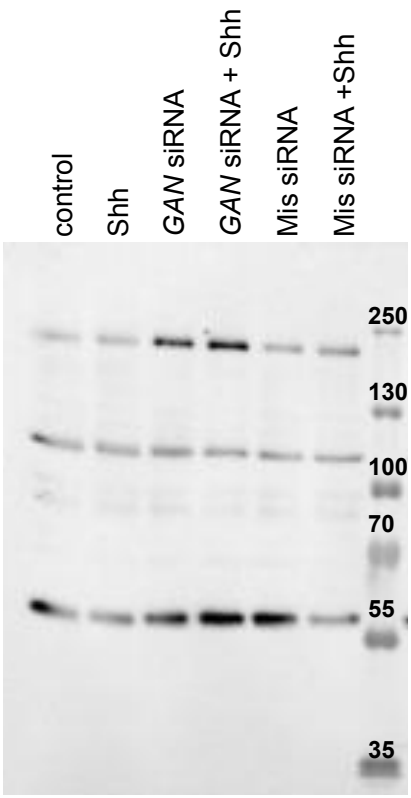

m-α-Ptch (1st antibody)
with ladder

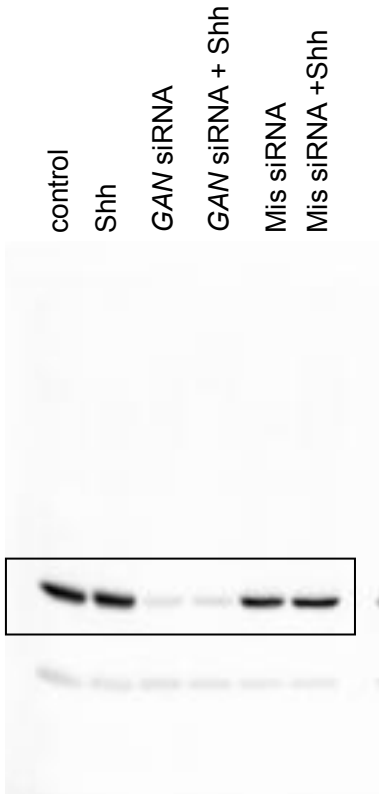

m-α-Gig (IId antibody)
w/o ladder

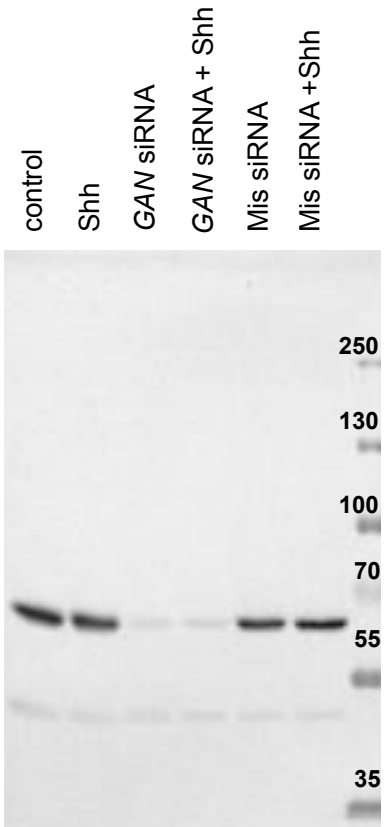

m-α-Gig with ladder

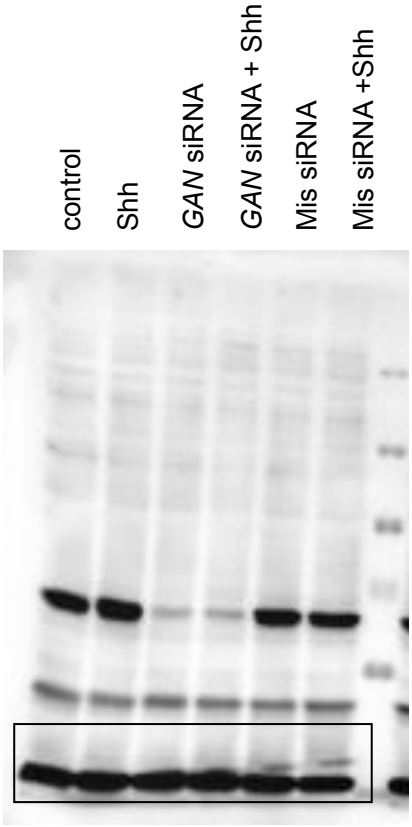

m- α-GAPDH (IIId antibody)

Full unedited gel for Figure 7 panel C

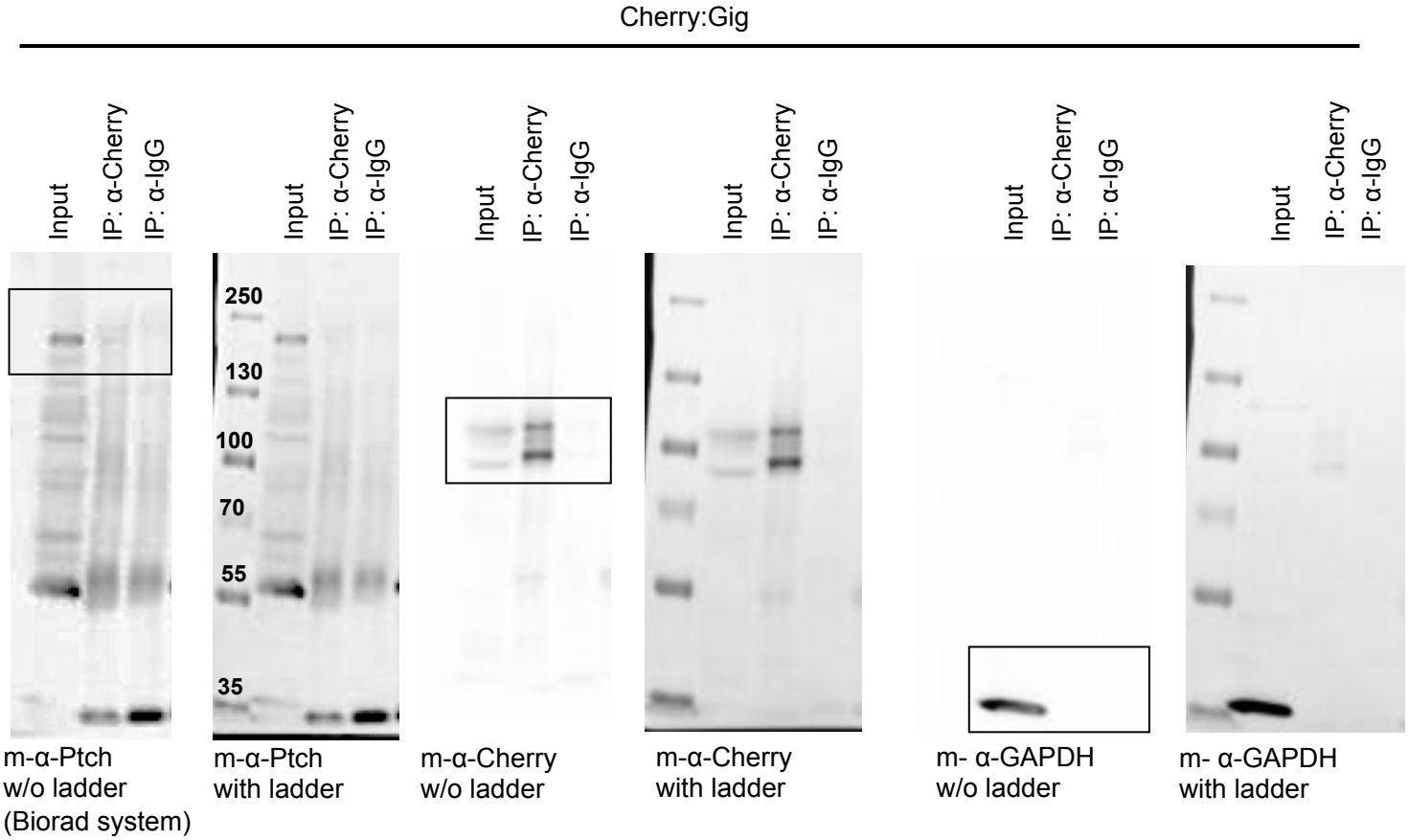

Full unedited gel for Figure 7 panel D

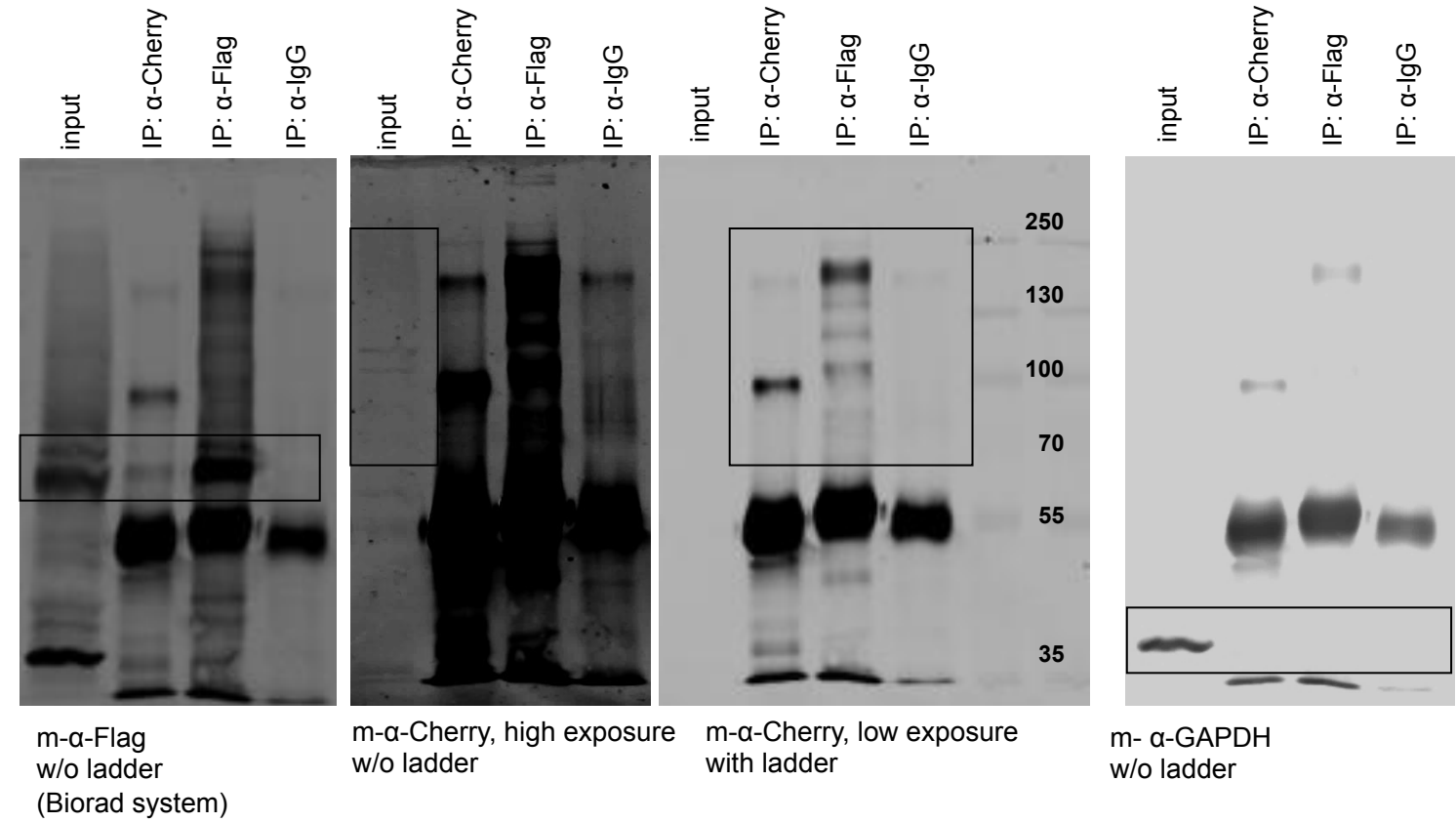

Full unedited gel for Figure 7 panel D

Cherry:Ptch+ Flag:Gig

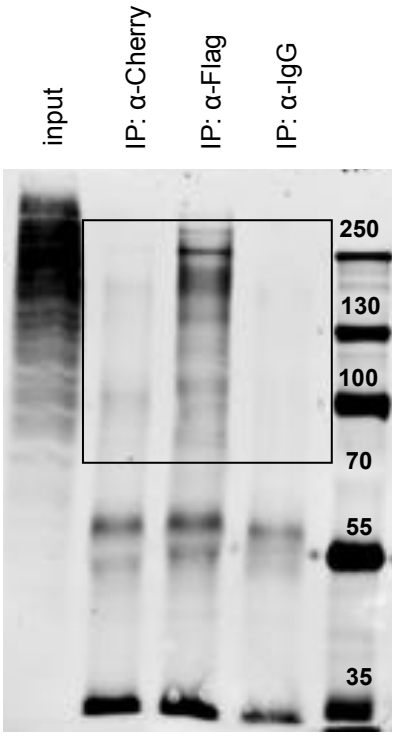

rb- α-K48
with ladder

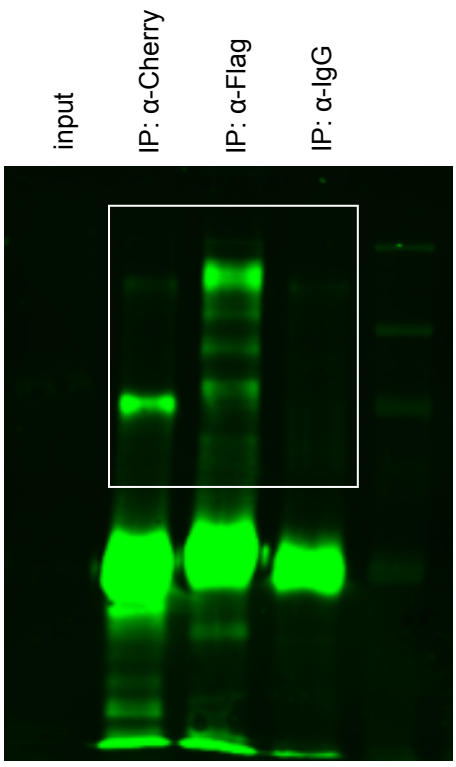

m- α-Cherry
(Licor system)

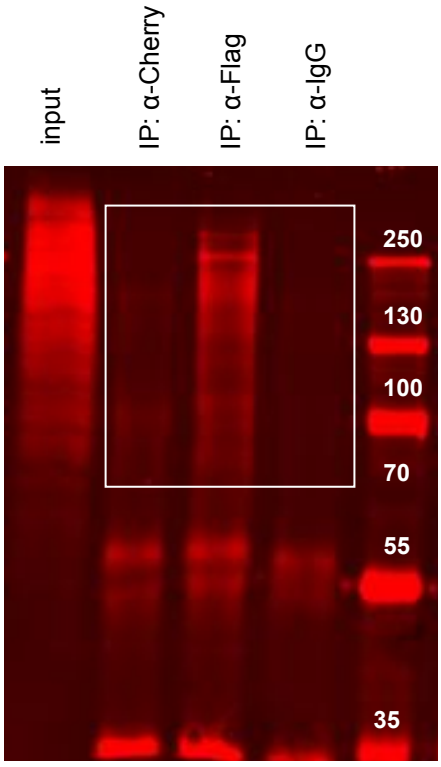

rb- α-K48

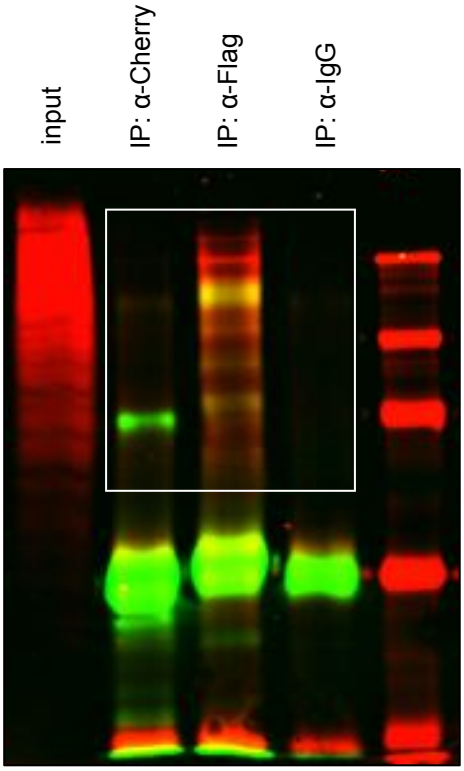

merge